GFZ

Helmholtz-Zentrum
POTSDAM

HELMHOLTZ-ZENTRUM POTSDAM
DEUTSCHES
GEOFORSCHUNGSZENTRUM

Scientific Technical Report STR

www.gfz-potsdam.de

HELMHOLTZ
GEMEINSCHAFT

Core-Mantle Coupling

Part II : Topographic coupling torques

Hans Greiner-Mai & Jan M. Hagedoorn

Scientific Technical Report 08/11 DOI: 10.2312/GFZ.b103-08113 Deutsches GeoForschungsZentrum GFZ

Table of Contents

Introduction | 1

1.1 Introduction to this Scientific Technical Report (STR)

For the motivation behind our investigations, we refer to the introduction of the first part of our report, Hagedoorn & Geiner-Mai (2008). In this part, we will (i) give an analytical description of the topographic surface of the core-mantle boundary (CMB) and derive an approximation for its normal unit vector containing information about the CMB topography, and (ii) derive an expression for the topographic torque as a function of the topographic height, h, and the velocity field, $\boldsymbol{u}$. For this, we will check the assumptions made when applying the geostrophic approximation to the upper core-surface region. Finally, we will derive analytical expressions for the torque components depending upon the spherical harmonic (SH) coefficients of h and $\boldsymbol{u}$ in a cartesian geocentric coordinate system.

The velocity field will be conventionally inferred from the poloidal geomagnetic field, $\boldsymbol{B}^{\mathrm{P}}$, at the CMB, or strictly speaking from its radial component, B_r^{P}, by inverting the so called frozen-field equation (see e.g. Backus, 1969), which is an approximation of the geomagnetic induction equation of the core valid for the decadal time scale considered here (10 to 100 years) and for spatial scales that are not too small (equivalent degree of SH expansion not larger than 10). The calculation of the topographic torque was the subject of several investigations in the past, e.g. Hinderer et al. (1987), Hide (1989), Jault & LeMouël (1989), Hide et al. (1996), and Asari et al. (2006). What is new from our investigation and outlined in this report, is that we infer $\boldsymbol{B}^{\mathrm{P}}$ at the CMB from the geomagnetic surface field by the non-harmonic downward continuation (NHDC) developed recently by Ballani et al. (2002) and discuss the role of the magnetic field and the Lorentz force in the geostrophic approximation on the basis of our newest results of the computation of the toroidal field, $\boldsymbol{B}^{\mathrm{T}}$, (Hagedoorn & Geiner-Mai, 2008). The velocity field needed for the torque calculation will be derived from this B_r-component (and its "secular variation" $\dot{B}_r$) according to Wardinski (2005), who used the geostrophic constraint to determine a $\boldsymbol{u}$-field, which is then in accordance with the above mentioned use of the geostrophic approximation for the torque computation. In this report, we will take the SH coefficients of the $\boldsymbol{u}$-field as given input data. The same applies to the SH coefficients of h, which we will take from literature (e.g. Morelli & Dziewonski, 1987; Sze & van der Hilst, 2003; Steinberger & Holme, 2008).

Another difference to previous investigations is that we use, consistent with part I of our report, the orthonormal SH base functions to derive analytical expressions of the torques. This requires us to determine some transformations between them and those representations used in geomagnetism (Ferrers-Neuman and Schmidt's normalization) that are given in appendix A.

1.2 Introduction to topographic core-mantle coupling

The topographic core-mantle coupling torque is produced by the mechanical interaction of the fluid flow of metallic core material with the CMB topography. The fluid flow relative to the solid mantle imposes (dynamic) pressure upon the topographic surface of the CMB, which accelerates the overlying mantle, resulting in the fluid flow losing angular momentum. From its physical nature, the topographic torque is, therefore, a pressure torque. For the atmosphere, the corresponding torque is also known as mountain torque, produced by pressure forces on mountains (as well as houses, trees etc.) when the wind blows towards them. For the core, the corresponding "mountains" are the so-called bumps of the CMB, the corresponding "metallic wind" is the fluid flow. Another mechanical coupling superimposed on this process, the friction, will conventionally be neglected because it is very small for the outer core (see e.g. Chap. 2.2).

The basic equations to be used for the atmosphere and liquid outer core are quite similar, but the approximations of them are based on other scales of the associated terms, in particular for the electromagnetic field and the related Lorentz force play a decisive role in the core but is negligible in the atmosphere. The pressure torque is described by a surface integral over the topographic surface, S, and the density of the pressure force, ∇p, acting on this topographic surface. This expression is derived by integrating the associated torque density $\boldsymbol{r} \times \nabla p$ over the volume, V, containing the liquid, and applying the integral theorem

$$\int\limits_{S} \boldsymbol{a} \times \mathrm{d}\boldsymbol{S} = -\int\limits_{V} \operatorname{rot} \boldsymbol{a} \, \mathrm{d}\boldsymbol{V}, \tag{1.1}$$

which is a version of the integral theorem of Gauss (e.g. Smirnov, 1964). The pressure torque described as surface and volume integral follows if we set $\boldsymbol{a} = \boldsymbol{r}\, p_u$ and use $\operatorname{rot} \boldsymbol{r}\, p_u = -\boldsymbol{r} \times \nabla p_u$.

With respect to the sign used in the definitions, we find no standard rule in the literature (compare e.g. Hide (1989) with Jault & LeMouël (1989)). The sign in fact seems to depend on whether the ∇p-term appears on the right-hand or left-hand side in the individual notations of the Navier Stokes equation. Therefore, it is important when comparing the different types of torques to check which sign will appear on the "torque side" in the respective notation. Here, we will follow Hide's notation (e.g. Hide, 1989) who introduces the torque independent of the equation in which it appears with $+\nabla\, p_u$.

In the following two chapters, we will re-examine and discuss some derivations of the final expression of the vectorial representation of the topographic torque in dependence on $\boldsymbol{u}$ and h. The motivation of this is to gain a better insight into some of the assumptions that are described in the literature as being self-evident. In chapter 2.3, we present the way and results of the derivation of the analytical expressions of the torque by SH coefficients of h and $\boldsymbol{u}$. Finally, we present in chapter 3 a simple example of topographic coupling for an ellipsoidal CMB and a non-axial rigid rotation of the fluid, know within other contexts as inertial coupling. Additional derivations are provided in the appendix A.

The topographic (TOP) core-mantle coupling torque | 2

2.1 TOP torque in dependence on the pressure gradient

In this report, we use for the topographic torque the symbol $\boldsymbol{L}$ without an additional index (like in part I for the EM torque). Following Sec. 1.2, the topographic coupling torque on the mantle is defined by

$$\boldsymbol{L} := \int\limits_{V_{\text{core}}} \boldsymbol{r} \times \nabla p_u \mathrm{d}V = - \int\limits_{V_{\text{core}}} \operatorname{rot}\big(\boldsymbol{r} p_u\big) \mathrm{d}V = \int\limits_{S_{\text{core}}} \boldsymbol{r} \times p_u \boldsymbol{n} \mathrm{d}S \tag{2.1}$$

where $\boldsymbol{n}$ is the outward normal unit vector on the CMB and p_u the dynamic pressure associated with core motions just below the CMB (bulk stream). The topographic or pressure torque is a part of the total torque on the mantle, caused by viscous ($\boldsymbol{f}_\nu$), electromagnetic ($\boldsymbol{f}_{\text{B}}$) and topographic ($\boldsymbol{f}_{\text{top}}$) stresses at the CMB

$$\boldsymbol{L}_{\text{CMB}} = \int\limits_{S_{\text{core}}} \boldsymbol{r} \times \big[\boldsymbol{f}_\nu + \boldsymbol{f}_{\text{B}} + \boldsymbol{f}_{\text{top}}\big] \mathrm{d}S, \tag{2.2}$$

and gravitational coupling between inner core and the mantle. The topographic stress is due to the action of normal pressure forces on bumps in the shape of the core-mantle interface, which are described by a suitable model of the departure of the CMB from a reference sphere. The magnetic stress is due to the Lorentz force on the mantle. The evaluation of the electromagnetic (EM) torque on the mantle is described in detail in Hagedoorn & Geiner-Mai (2008). From the viscous torque on the mantle, it is generally believed that its contribution to core-mantle coupling is marginal (e.g. Bullard et al., 1950), in contrast to its effect at the inner-core / outer-core boundary.

One major point in solving the integral in eq. (2.1) is to express $\boldsymbol{n}$ by a parameter defining the CMB topography. Let the CMB be described by the surface equation

$$\boldsymbol{r} = \boldsymbol{F}(\vartheta, \varphi) = \boldsymbol{e}_r\big(R_{\text{CMB}} + h(\vartheta, \varphi)\big), \tag{2.3}$$

where $h(\vartheta, \varphi)$ is the topographic height over a reference sphere (see Fig. 2.1), the radius of which is the mean core radius, R_{CMB}, and r, ϑ, φ are the spherical coordinates. The normal vector $\boldsymbol{N}$ on $\boldsymbol{F}$ is then given by the vector product of the derivations of $\boldsymbol{F}(\vartheta, \varphi)$ (tangential vectors) to its parameters (e.g. Heuser, 1993, p. 503-504)

$$\boldsymbol{N} = \frac{\partial \boldsymbol{F}}{\partial \vartheta} \times \frac{\partial \boldsymbol{F}}{\partial \varphi}\,. \tag{2.4}$$

From eq. (2.3) follows that

$$\frac{\partial \boldsymbol{F}}{\partial \vartheta} = \frac{\partial \boldsymbol{e}_r}{\partial \vartheta}\, \big[R_{\text{CMB}} + h(\vartheta, \varphi)\big] \, + \boldsymbol{e}_r \, \frac{\partial [R_{\text{CMB}} + h(\vartheta, \varphi)]}{\partial \vartheta}\,, \tag{2.5}$$

$$\frac{\partial \boldsymbol{F}}{\partial \varphi} = \frac{\partial \boldsymbol{e}_r}{\partial \varphi}\, \big[R_{\text{CMB}} + h(\vartheta, \varphi)\big] \, + \boldsymbol{e}_r \, \frac{\partial [R_{\text{CMB}} + h(\vartheta, \varphi)]}{\partial \varphi}, \tag{2.6}$$

with

$$\frac{\partial \boldsymbol{e}_r}{\partial \vartheta} = \boldsymbol{e}_\vartheta, \qquad \frac{\partial \boldsymbol{e}_r}{\partial \varphi} = \sin\vartheta\, \boldsymbol{e}_\varphi, \tag{2.7}$$

where $\boldsymbol{e}_{\dots}$ denotes the unit vectors in spherical coordinates we obtain for the normal vector $\boldsymbol{N}$ according

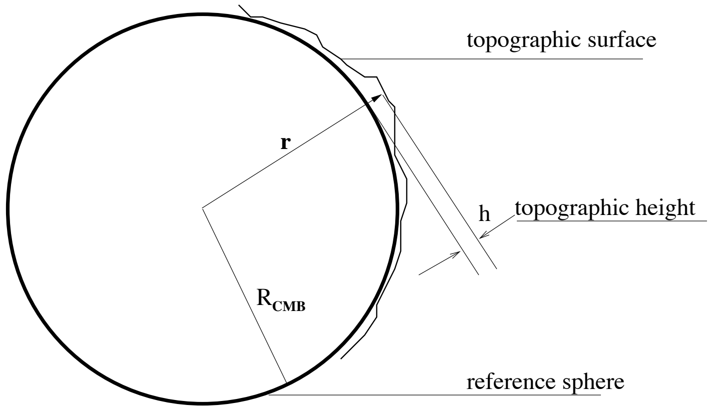

Figure 2.1: Schematic illustration of the topographic surface and its parameters ($\boldsymbol{r}$ = position vector, R_{CMB} = mean core radius)

to eqs. (2.4) to (2.6), leading to

$$\begin{aligned}\boldsymbol{N} = &\, \boldsymbol{e}_r \left[R_{\text{CMB}} + h(\vartheta,\varphi)\right]^2 \sin\vartheta \\ &- \boldsymbol{e}_\vartheta \left[R_{\text{CMB}} + h(\vartheta,\varphi)\right] \sin\vartheta \, \frac{\partial h}{\partial \vartheta} \\ &- \boldsymbol{e}_\varphi \left[R_{\text{CMB}} + h(\vartheta,\varphi)\right] \frac{\partial h}{\partial \varphi}. \end{aligned} \tag{2.8}$$

To calculate the unit vector $\boldsymbol{n}$ in eq. (2.1), we first must calculate the absolute value of $\boldsymbol{N}$. For this, we rewrite eq. (2.8) as

$$\frac{1}{R_{\text{CMB}}^2}\boldsymbol{N} = \boldsymbol{e}_r \left[1+a\right]^2 \sin\vartheta - \boldsymbol{e}_\vartheta \left[1+a\right] \sin\vartheta \, \frac{1}{R_{\text{CMB}}} \frac{\partial h}{\partial \vartheta} - \boldsymbol{e}_\varphi \left[1+a\right] \frac{1}{R_{\text{CMB}}} \frac{\partial h}{\partial \varphi} \tag{2.9}$$

with $a = h/R_{\text{CMB}}$.

If we assume a maximum topographic height, h, of $10\,$km, then $a \approx 0.003$. Furthermore, the change of h with ϑ and φ cannot exceed the maximum value of h so that $R_{\text{CMB}}^{-1} \cdot [\partial h/\partial(\vartheta,\varphi)] \leq a$. The absolute value, N, of $\boldsymbol{N}$ according to eq. (2.9), can then be approximated by $R_{\text{CMB}}^2 \sin\vartheta$, and the normal unit vector by

$$\boldsymbol{n} = \frac{\boldsymbol{N}}{N} = \boldsymbol{e}_r - \boldsymbol{e}_\vartheta \frac{1}{R_{\text{CMB}}} \frac{\partial h}{\partial \vartheta} - \boldsymbol{e}_\varphi \frac{1}{R_{\text{CMB}} \sin\vartheta} \frac{\partial h}{\partial \varphi} = \boldsymbol{e}_r - \nabla_{\text{H}}\, h. \tag{2.10}$$

Note that the definition of ∇_{H} used here contains R_{CMB}^{-1}. The topographic torque (2.1) is then written as

$$\boldsymbol{L} = -R_{\text{CMB}}^2 \int_\Omega \left(\boldsymbol{r} \times p_u \nabla_{\text{H}} h\right) \mathrm{d}\Omega, \tag{2.11}$$

where $\Omega = (\vartheta, \varphi)$ and $\mathrm{d}\Omega$ denote the infinitesimal surface element $\sin\vartheta\, \mathrm{d}\vartheta \mathrm{d}\varphi$ in spherical coordinates. The dynamic pressure is determined by the Navier-Stokes equation, where its gradient appears. Therefore, we will shift the ∇-term in eq. (2.11) from h to p_u by partial integration,

$$\boldsymbol{L} = -R_{\text{CMB}}^2 \int_\Omega \left[\boldsymbol{r} \times \nabla_{\text{H}}(p_u\, h)\right] \mathrm{d}\Omega + R_{\text{CMB}}^2 \int_\Omega \left[\boldsymbol{r} \times h\, (\nabla_{\text{H}} p_u)\right] \mathrm{d}\Omega. \tag{2.12}$$

It can be shown that the first integral in (2.12) vanishes: The implementation of the vectorial product, $\boldsymbol{r} \times \nabla_{\text{H}}(p_u h)$, gives

$$\begin{aligned} &- R_{\text{CMB}}^2 \int_\Omega \left(- \boldsymbol{e}_\vartheta \frac{1}{\sin\vartheta} \frac{\partial}{\partial\varphi}(p_u\, h) + \boldsymbol{e}_\varphi \frac{\partial}{\partial\vartheta}(p_u\, h) \right) \mathrm{d}\Omega = \\ &- R_{\text{CMB}}^2 \int_\Omega \left[-\frac{\partial}{\partial\varphi}\left(\frac{\boldsymbol{e}_\vartheta p_u h}{\sin\vartheta}\right) + \frac{p_u h}{\sin\vartheta} \frac{\partial \boldsymbol{e}_\vartheta}{\partial\varphi} + \frac{\partial(\boldsymbol{e}_\varphi p_u h)}{\partial\vartheta} - p_u h \frac{\partial \boldsymbol{e}_\varphi}{\partial\vartheta} \right] \mathrm{d}\Omega\,, \end{aligned}$$

where

$$\frac{\partial \boldsymbol{e}_\vartheta}{\partial \varphi} = \cos\vartheta\, \boldsymbol{e}_\varphi, \quad \frac{\partial \boldsymbol{e}_\varphi}{\partial \vartheta} = 0.$$

It therefore follows that

$$- R^2_{\text{CMB}} \int\limits_0^{2\pi} \int\limits_0^{\pi} \left[-\frac{\partial(\boldsymbol{e}_\vartheta p_u\, h)}{\partial \varphi} + p_u\, h\, \cos\vartheta\, \boldsymbol{e}_\varphi + \sin\vartheta \frac{\partial(\boldsymbol{e}_\varphi p_u\, h)}{\partial \vartheta} \right] \mathrm{d}\vartheta\, \mathrm{d}\varphi =$$

$$- R^2_{\text{CMB}} \int\limits_0^{2\pi} \int\limits_0^{\pi} \left[-\frac{\partial(\boldsymbol{e}_\vartheta p_u h)}{\partial \varphi} + \frac{\partial(\sin\vartheta\, \boldsymbol{e}_\varphi p_u\, h)}{\partial \vartheta} \right] \mathrm{d}\vartheta\, \mathrm{d}\varphi = 0\,, \tag{2.13}$$

since the first product in parentheses in the integral (2.13) is unique, i.e. equal at $\varphi = 0, 2\pi$, and the second one vanishes because $\sin\vartheta$ vanishes at $\vartheta = 0, \pi$.

From eq. (2.12), we can now derive the final expression

$$\boldsymbol{L} = R^2_{\text{CMB}} \int\limits_\Omega \left[\boldsymbol{r} \times h\, (\nabla_{\text{H}} p_u) \right] \mathrm{d}\Omega. \tag{2.14}$$

2.2 The geostrophic balance

The hydrodynamical equation of motions within the core (Navier-Stokes equation) is given by

$$\rho\,\frac{\partial \boldsymbol{u}}{\partial t} + \rho\,[\boldsymbol{u}\cdot\nabla]\boldsymbol{u} + 2\rho\,\boldsymbol{\omega}\times\boldsymbol{u} + \nabla p - \rho\boldsymbol{g} = \boldsymbol{j}\times\boldsymbol{B} + \nu\rho\nabla^2\boldsymbol{u}, \tag{2.15}$$

where ρ denotes the density, ν the dynamic viscosity, p the total pressure, $\boldsymbol{u}$ the Eulerian velocity in a frame of reference that rotates with an angular velocity $\boldsymbol{\omega}$ relative to an inertial frame, and $\boldsymbol{g}$ is the gravitational acceleration. In eq. (2.15), the centrifugal force is included in ∇p.

According to e.g. Hide (1989), eq. (2.15) can be approximated by

$$2\rho\,\boldsymbol{\omega}\times\boldsymbol{u} + \nabla p - \boldsymbol{g}\rho \approx \boldsymbol{j}\times\boldsymbol{B}, \tag{2.16}$$

if the relative acceleration terms and the viscous term are negligible. Hereafter, we will give our own reasoning to this. Over decadal time scale (10 years), for spatial dimensions of the core radius (3485 km), for velocities known from frozen-flux approximations of the geomagnetic secular variation (about 10 km a^{-1}) and for an upper bound of the viscosity ($10^{-2}\times$ m^{2}s^{-1}; Mound & Buffett, 2007), the acceleration, the viscous and the Coriolis terms have order of magnitude values ($\mathcal{O}$) of

$$\mathcal{O}\big(\rho\,\frac{\partial \boldsymbol{u}}{\partial t}\big) = 1.0\times10^{-12}\,\mathrm{m\,s^{-2}}\;\times\;\mathcal{O}(\rho), \tag{2.17}$$

$$\mathcal{O}\big(\rho\,[\boldsymbol{u}\cdot\nabla]\boldsymbol{u}\big) = 2.9\times10^{-14}\,\mathrm{m\,s^{-2}}\;\times\;\mathcal{O}(\rho), \tag{2.18}$$

$$\mathcal{O}\big(\nu\rho\,\nabla^2\boldsymbol{u}\big) = 1.1\times10^{-20}\,\mathrm{m\,s^{-2}}\;\times\;\mathcal{O}(\rho), \tag{2.19}$$

$$\mathcal{O}\big(2\rho\,\boldsymbol{\omega}\times\boldsymbol{u}\big) = 4.6\times10^{\;-8}\,\mathrm{m\,s^{-2}}\;\times\;\mathcal{O}(\rho), \tag{2.20}$$

where $\mathcal{O}(\rho)$ is the order of magnitude of the volume mass density. This comparison shows that the acceleration and viscous terms can be neglected compared with the Coriolis term.

The density of the Lorentz force, $\boldsymbol{j}\times\boldsymbol{B}$ ($\boldsymbol{j}$ is the density of electric currents, $\boldsymbol{B}$ is the magnetic flux), on the rhs of eq. (2.16) is not marginal and its magnitude depends on the strength of the magnetic field, which is not completely known at the top of the core, in particular the strength of its toroidal part. Recent investigations of EM coupling (e.g. Greiner-Mai et al., 2003) argue for an electric conductivity, σ_{M}, of the mantle (at least close to the CMB) of the same order of magnitude than that of the core. Therefore, the induced electric currents, $\boldsymbol{j}$, are not negligible. We will show such difficulties by a scaling consideration. A rough estimate of the poloidal magnetic field, $\boldsymbol{B}^{\mathrm{P}}$, gives a maximum value of the order of 1 mT at the CMB (e.g. Ballani et al., 2002). Taking for $\boldsymbol{j}$ the Maxwell equation $\boldsymbol{j} = \mu^{-1}\,\mathrm{rot}\,\boldsymbol{B}^{\mathrm{P}}$, scaling the rot by R_{CMB}^{-1}, and assuming for the core a density of the order of 10 g cm^{-3} we obtain with $\mu = 4\,\pi 10^{-7}$Vs(Am)$^{-1}$

$$\begin{aligned}\mathcal{O}\big(\mu^{-1}\,[\mathrm{rot}\,\boldsymbol{B}^{\mathrm{P}}]\times\boldsymbol{B}^{\mathrm{P}}\big) &= 2.3\times10^{-10}\,\mathrm{ms^{-2}\,g\,cm^{-3}}\\ &= 2.3\times10^{-11}\,\mathrm{ms^{-2}}\;\times\;\mathcal{O}(\rho).\end{aligned} \tag{2.21}$$

Therefore, the effect of the poloidal part of the magnetic field is marginal compared to that of the Coriolis force. For a weak-field dynamo, this is also true if the toroidal field, $\boldsymbol{B}^{\mathrm{T}}$, is involved (for this type of dynamo, $\boldsymbol{B}^{\mathrm{T}}$ is of the order of $\boldsymbol{B}^{\mathrm{P}}$). For a strong-field dynamo, the toroidal field can exceed the poloidal one by two orders of magnitude. So the combination $(\mathrm{rot}\,\boldsymbol{B}^{\mathrm{T}})\times\boldsymbol{B}^{\mathrm{P}}$ is only one order lower than the Coriolis term, but the combination $(\mathrm{rot}\,\boldsymbol{B}^{\mathrm{T}})\times\boldsymbol{B}^{\mathrm{T}}$ can exceed it. Due to our poor knowledge of the actual field strength of $\boldsymbol{B}^{\mathrm{T}}$, the relevance of the Lorentz term in eq. (2.16) is uncertain, and to omit it is only correct for particular models of the toroidal field.

To be in accordance with conventional procedures of approximation, we will bring another argument into play. In Hagedoorn & Geiner-Mai (2008), the variation of the toroidal field caused by the electromotive force $\boldsymbol{u}\times\boldsymbol{B}$ is evaluated to be less than the poloidal field. These variations are then consistent with the frozen-field approximation of the secular variation of the poloidal field; the associated currents have the same electric source field $\boldsymbol{E} = \boldsymbol{u}\times\boldsymbol{B}$. The variations of both fields (for $\boldsymbol{B}^{\mathrm{T}}$ the modelled), are then determined at the same level of approximation as the dynamic pressure p_u, i.e. if we attribute the tangential geostrophic equation (e.g. eq. (2.25)) to the dynamic part of the full problem, and consider the stationary part (with a much larger toroidal field) of the equation as a reference state (like hydrostatic equilibrium), then the neglecting of the Lorentz force is reasonable.

By neglecting the Lorentz term, from eq. (2.16) it follows that

$$2\rho\,\boldsymbol{\omega}\times\boldsymbol{u} = -\nabla p + \boldsymbol{g}\rho. \tag{2.22}$$

Assuming

$$\boldsymbol{\omega}\approx\omega\boldsymbol{e}_z, \qquad 2\rho\,\omega\boldsymbol{e}_z\times\boldsymbol{u}\approx -\nabla p + \boldsymbol{g}\rho, \tag{2.23}$$

we explicitly obtain

$$\begin{aligned} 2\rho\omega(u_\vartheta\,\cos\vartheta - u_r\,\sin\vartheta) &= -\frac{1}{r\,\sin\vartheta}\frac{\partial p}{\partial\varphi} + \rho g_\varphi,\\ 2\rho\omega u_\varphi\,\cos\vartheta &= \frac{1}{r}\frac{\partial p}{\partial\vartheta} - \rho g_\vartheta,\\ 2\rho\omega u_\varphi\,\sin\vartheta &= -\frac{1}{r}\frac{\partial p}{\partial r} + \rho g_r. \end{aligned} \tag{2.24}$$

The non-penetration condition at the CMB reads as $\boldsymbol{u}\cdot\boldsymbol{n}=0$, from which follows according to eq. (2.10) $u_r - \boldsymbol{u}\nabla_{\mathrm{H}}h = 0$, where $u_r = \boldsymbol{u}\nabla_{\mathrm{H}}h$. The gradient $\nabla_{\mathrm{H}}h$ is of the order of 3×10^{-3} and it is $\mathcal{O}(u_r) = 3\times10^{-3}\mathcal{O}(\boldsymbol{u}_{\mathrm{H}})$. Therefore, the u_r-term can be neglected compared with the u_ϑ-term in the first eq. (2.24). It is usually assumed that $\boldsymbol{g}$ points in $\boldsymbol{e}_r$ direction, i.e. (g_ϑ, g_φ) can also be neglected. The remaining approximation is the conventional geostrophic equation, the horizontal part of which describes the so-called tangential geostrophy

$$\begin{aligned} 2\rho\,\omega\,u_\vartheta\,\cos\vartheta &= -\frac{1}{r\,\sin\vartheta}\frac{\partial p}{\partial\varphi},\\ 2\rho\,\omega\,u_\varphi\,\cos\vartheta &= \frac{1}{r}\frac{\partial p}{\partial\vartheta}, \end{aligned} \tag{2.25}$$

whereas the last equation of (2.24) leads to the hydrostatic equation, obtained by leaving the u_φ-term ($\omega\,u_\varphi$ is of the order of 10^{-9} m s^{-2}, i.e. much smaller than g_r). With the Coriolis parameter, f, eqs. (2.25) can be written as

$$f\,\boldsymbol{u}_{\mathrm{H}} = \boldsymbol{e}_r\,\times\,\nabla p = -\,\mathrm{rot}(\boldsymbol{e}_r p), \qquad f = 2\rho\omega\cos\vartheta, \tag{2.26}$$

from which follows $\mathrm{div}(f\,\boldsymbol{u}_{\mathrm{H}}) = 0$. Assuming that the density variations are insignificant in the CMB region considered, i.e. $\rho=\bar\rho$, from this divergence condition follows the geostrophic constraint

$$\mathrm{div}(\cos\vartheta\,\boldsymbol{u}_{\mathrm{H}}) = 0 \tag{2.27}$$

usually used as a dynamic constraint in the inversion of the frozen-field equation of the core motions for $\boldsymbol{u}$ in geomagnetism. Eq. (2.25) can be rewritten as

$$\nabla_{\mathrm{H}}p = -f\,\boldsymbol{e}_r\times\boldsymbol{u}_{\mathrm{H}}. \tag{2.28}$$

The relation of $\nabla_{\mathrm{H}}p$, e.g. in eq. (2.28), to the fluid motions of the core allows us to identify p with the dynamic pressure p_u of eq. (2.1), if ∇_{H} is applied.

With eqs. (2.28) and (2.14), the topographic torque can be written as an integral about $\boldsymbol{u}$ and $h(\vartheta,\varphi)$

$$\boldsymbol{L} = R^3_{\mathrm{CMB}}\int\limits_{\Omega} f(\vartheta)\,h(\vartheta,\varphi)\,\boldsymbol{u}_{\mathrm{H}}(R_{\mathrm{CMB}},\vartheta,\varphi,t)\,\mathrm{d}\Omega, \tag{2.29}$$

which we can also find in e.g. Hide (1989).

Now, we will summarize the assumptions necessary to derive eq. (2.28), used to express ∇p in eq. (2.14) by $\boldsymbol{u}$. The following terms of the Navier-Stokes equation are neglected compared with the Coriolis force

1. the Lorentz term;

2. the acceleration terms;

3. the friction term;

from which the first cannot be neglected generally, but is insignificant in the dynamic part of the problem. Further assumptions made are

a) $\boldsymbol{\omega}$ points in z-direction;

b) u_r is negligible compared with $\boldsymbol{u}_{\mathrm{H}}$;

c) the vector of gravitational acceleration, $\boldsymbol{g}$, points in r-direction;

d) the density variation along the CMB is negligible;

e) in eq. (2.10), ∇_{H} is applied for the reference sphere, $r = R_{\mathrm{CMB}}$. By the definition of the torque in eq. (2.1), it should be related to the real CMB, i.e. $R_{\mathrm{CMB}} + h$

Some of the used approximations/assumptions are well reasoned by scaling considerations, while some of them are made without quantitative reasoning, i.e. for plausibility only.

 DOI: 10.2312/GFZ.b103-08113

2.3 The componental form of the TOP torque

Using the relations between unit vectors in cartesian and spherical coordinates,

$$\begin{aligned}
\boldsymbol{e}_x &= \boldsymbol{e}_r\,\sin\vartheta\,\cos\varphi - \boldsymbol{e}_\varphi\,\sin\varphi + \boldsymbol{e}_\vartheta \cos\vartheta\,\cos\varphi,\\
\boldsymbol{e}_y &= \boldsymbol{e}_r\,\sin\vartheta\,\sin\varphi + \boldsymbol{e}_\varphi\,\cos\varphi + \boldsymbol{e}_\vartheta\,\cos\vartheta\,\sin\varphi,\\
\boldsymbol{e}_z &= \boldsymbol{e}_r\,\cos\vartheta - \boldsymbol{e}_\vartheta\,\sin\vartheta,
\end{aligned} \tag{2.30}$$

and assuming $\rho = \bar{\rho}$ = const., we obtain for the components of the torque

$$\begin{aligned}
L_x &= a \int\limits_\Omega h\,(u_\vartheta\,\cos\vartheta\,\cos\varphi - u_\varphi\,\sin\varphi)\,\cos\vartheta\,\mathrm{d}\Omega\\
L_y &= a \int\limits_\Omega h\,(u_\vartheta\,\cos\vartheta\,\sin\varphi + u_\varphi\,\cos\varphi)\,\cos\vartheta\,\mathrm{d}\Omega\\
L_z &= -a \int\limits_\Omega h\,u_\vartheta\,\cos\vartheta\,\sin\vartheta\,\mathrm{d}\Omega
\end{aligned} \tag{2.31}$$

$$a = 2\,\bar{\rho}\,\omega\,R^3_{\text{CMB}}. \tag{2.32}$$

It is easily shown that the equatorial components can be combined into one complex torque, $L = L_x + i\,L_y$, given by

$$L = a \int\limits_\Omega h\,(u_\vartheta\,\cos\vartheta + i\,u_\varphi)\,e^{i\varphi}\,\cos\vartheta\,\mathrm{d}\Omega, \qquad i = \sqrt{-1}\,. \tag{2.33}$$

For later numerical estimates of the torque, we will use values of $\boldsymbol{u}_\text{H}$ inferred by Wardinski (2005) from the C^{3}FM geomagnetic field (Wardinski & Holme, 2006). Therefore, we will decompose the velocity field in a manner consistent with these investigations. Assuming $\nabla\boldsymbol{u} = 0$, Wardinski (2005) decomposed $\boldsymbol{u}_\text{H}$ into poloidal and toroidal parts

$$u^\text{P} = \nabla_\text{H}(rP) = \left(0,\,\frac{\partial P}{\partial\vartheta},\,\frac{1}{\sin\vartheta}\frac{\partial P}{\partial\varphi}\right), \tag{2.34}$$

$$u^\text{T} = \nabla_\text{H}\,\times\,(\boldsymbol{r}Q) = \left(0,\,\frac{1}{\sin\vartheta}\frac{\partial Q}{\partial\varphi},\,-\frac{\partial Q}{\partial\vartheta}\right), \tag{2.35}$$

where $P(r,\vartheta,\varphi,t)$ and $Q(r,\vartheta,\varphi,t)$ are the defining scalar functions of the poloidal (superscript P) and toroidal (superscript T) part of the velocity field, respectively. It should be mentioned that this decomposition for the horizontal velocity field also follows for the general case $\nabla\boldsymbol{u} \neq 0$, for which the general decomposition is given by Krause & Rädler (1980)

$$\boldsymbol{u} = \nabla\,\times\,(\boldsymbol{r}Q) + \boldsymbol{r}V + \nabla\,W, \tag{2.36}$$

if we set $W = r\,P$.

Inserting eqs. (2.34) and (2.35) into the torque expressions (2.31) and (2.33), we obtain the torque components as a function of h and these defining scalars

$$L^\text{T} = a \int\limits_\Omega h\left[\cot\vartheta\,\frac{\partial Q}{\partial\varphi} - i\,\frac{\partial Q}{\partial\vartheta}\right] e^{i\varphi}\,\cos\vartheta\,\mathrm{d}\Omega, \tag{2.37}$$

$$L^\text{P} = a \int\limits_\Omega h\left[\cos\vartheta\,\frac{\partial P}{\partial\vartheta} + i\,\frac{1}{\sin\vartheta}\frac{\partial P}{\partial\varphi}\right] e^{i\varphi}\,\cos\vartheta\,\mathrm{d}\Omega, \tag{2.38}$$

$$L^\text{T}_z = -\,a \int\limits_\Omega h\,\frac{\partial Q}{\partial\varphi}\,\cos\vartheta\,\mathrm{d}\Omega, \tag{2.39}$$

$$L^\text{P}_z = -\,a \int\limits_\Omega h\,\sin\vartheta\,\frac{\partial P}{\partial\vartheta}\,\cos\vartheta\,\mathrm{d}\Omega. \tag{2.40}$$

To obtain the torque in terms of the spherical harmonic (SH) coefficients of the fields P, Q, h, we use the fully normalized spherical harmonic functions described in Hagedoorn & Geiner-Mai (2008) [see also Appendix A],

$$Y_{jm}(\Omega) := P_{jm}(\cos\vartheta)\, e^{i\,m\varphi}, \tag{2.41}$$

where P_{jm} are the associated Legendre polynomials and $\Omega = (\vartheta, \varphi)$. The used coefficients are defined by the SH expansion of P, Q, h

$$P = \sum_{jm} p_{jm}(t) Y_{jm}(\Omega), \quad Q = \sum_{jm} q_{jm}(t) Y_{jm}(\Omega), \quad h = \sum_{jm} h_{jm} Y_{jm}(\Omega), \tag{2.42}$$

where it is assumed that the topographic height is independent of the time t over the time scales of interest to this study. The torque components are then given by

$$L^{\mathsf{T}} = \quad a \sum_{jm}\sum_{kl} i\, q_{jm} h_{lk} \int_{\Omega} Y_{lk} \left[m\, \cot\vartheta\, Y_{jm} - \frac{\partial}{\partial\vartheta} Y_{jm} \right] e^{i\,\varphi}\, \cos\vartheta\, \mathrm{d}\Omega \tag{2.43}$$

$$L^{\mathsf{P}} = \quad a \sum_{jm}\sum_{kl} p_{jm} h_{lk} \int_{\Omega} Y_{lk} \left[\cos\vartheta\, \frac{\partial}{\partial\vartheta} Y_{jm} - \frac{m}{\sin\vartheta}\, Y_{jm} \right] e^{i\,\varphi}\, \cos\vartheta\, \mathrm{d}\Omega \tag{2.44}$$

$$L_z^{\mathsf{T}} = -\, a \sum_{jm}\sum_{kl} i\, m\, q_{jm} h_{lk} \int_{\Omega} \cos\vartheta\, Y_{lk}\, Y_{jm}\, \mathrm{d}\Omega \tag{2.45}$$

$$L_z^{\mathsf{P}} = -\, a \sum_{jm}\sum_{kl} p_{jm} h_{lk} \int_{\Omega} \cos\vartheta\, \sin\vartheta\, Y_{lk} \frac{\partial}{\partial\vartheta} Y_{jm}\, \mathrm{d}\Omega \tag{2.46}$$

To solve the integrals in eqs. (2.43)-(2.46), we require a recurrence formulae for the SH expressions in them and the normalization condition of the spherical harmonics. For the related derivations, we refer the reader to the Appendix A. Below, we will give the resulting analytical expressions for the torques.

To solve the integrals in the z components, we need the relations (A.9) and (A.12) derived in Appendix A, and apply the normalization condition (A.2) and the complex conjugate (A.3). We obtain for these torque components

$$L_z^{\mathsf{T}} = -i\, a \sum_{j=1}^{J} \sum_{m=-j}^{+j} m\, (-1)^m q_{jm} \left[h_{(j+1)(-m)} \sqrt{\frac{(j+1)^2 - m^2}{(2j+1)(2j+3)}} + h_{(j-1)(-m)} \sqrt{\frac{j^2 - m^2}{(2j+1)(2j-1)}} \right] \tag{2.47}$$

$$L_z^{\mathsf{P}} = -a \sum_{j=1}^{J} \sum_{m=-j}^{+j} (-1)^m\, p_{jm} \left[\frac{j\, h_{(j+2)(-m)}}{2j+3} \sqrt{\frac{[(j+2)^2 - m^2][(j+1)^2 - m^2]}{(2j+1)(2j+5)}} - \frac{(j+1)\, h_{(j-2)(-m)}}{2j-1} \right.$$
$$\left. \sqrt{\frac{[j^2 - m^2][(j-1)^2 - m^2]}{(2j+1)(2j-3)}} + \frac{h_{j(-m)}}{2j+1} \left(\frac{j[(j+1)^2 - m^2]}{(2j+3)} - \frac{(j+1)(j^2 - m^2)}{(2j-1)} \right) \right]. \tag{2.48}$$

It can be seen that for $j = 1$ negative degrees in $h_{(j-2)\,m}$ are excluded by the numerator under the square root. The SH expansions for h and the defining scalars of $\boldsymbol{u}$ begin with $j = 1$, while the index in in $h_{(j-2)m}$ becomes zero for $j = 2$. To solve this problem and that with the upper bound of summation is a matter of implementation (the negative index $-m$ can be removed by e.g. an index transformation $m := -q$).

The analytical expressions for the equatorial torques is obtained in similar manner from eqs. (A.14) and (A.20):

$$L^{\mathsf{T}} = i\,a \sum_{j=1}^{J} \sum_{m=-j}^{+j} (-1)^m\, q_{jm} \left[(j-m) h_{(j+1)(-m-1)} \sqrt{\frac{(j+m+2)(j+m+1)}{(2j+1)(2j+3)}} \right.$$
$$\left. + (j+m+1) h_{(j-1)(-m-1)} \sqrt{\frac{(j-m)(j-m-1)}{(2j+1)(2j-1)}} \right] \tag{2.49}$$
$$L^{\mathsf{P}} = -\,a \sum_{j=1}^{J} \sum_{m=-j}^{+j} (-1)^m\, p_{jm} \left[\frac{j\, h_{(j+2)(-m-1)}}{2j+3} \sqrt{\frac{[(j+1)^2-m^2][j+m+2][j+m+3]}{(2j+1)(2j+5)}} \right.$$
$$+ \frac{(j+1)\, h_{(j-2)(-m-1)}}{2j-1} \sqrt{\frac{[j^2-m^2][j-m-1][j-m-2]}{(2j+1)(2j-3)}}$$
$$\left. + \frac{\sqrt{(j-m)(j+m+1)}\, h_{j(-m-1)}}{2j+1} \left(\frac{j(j+m+2)}{2j+3} + \frac{(j+1)(j-m-1)}{2j-1} \right) \right]. \tag{2.50}$$

In eq. (2.50), the second term becomes zero for $j = 2, 1,$ and 0. It is important for the numerical implementation of these expressions that h and $\boldsymbol{u}$ are given as real functions and their SH coefficients are related to non-orthonormal SH base functions in Ferrers-Neumann and Schmidt's normalization. The related transformation of the SH coefficients are described in Part I (Hagedoorn & Geiner-Mai, 2008), and the implementation of them is already completed in connection with the computation of the EM coupling torques.

First application for a non-axially rotating core fluid in an ellipsoid | 3

To obtain some idea about the order of magnitude of the topographic torque, we will derive an analytical expression for the example of a fluid rotating rigidly within an ellipsoidal surface. The rotation of the fluid can be interpreted as the first order of the SH harmonic expansion of a toroidal velocity field. The pure toroidal property can be proved by the relation:

$$\boldsymbol{u} = \boldsymbol{\varpi} \times \boldsymbol{r} = \mathrm{rot}\,\boldsymbol{r}(\boldsymbol{r}\cdot\boldsymbol{\varpi}) \tag{3.1}$$

where $\boldsymbol{\varpi} = (\varpi_x, \varpi_y, \varpi_z)$ is the vector of the angular velocity of the fluid in a mantle-fixed coordinate system, i.e. that of its rotation relative to the mantel. The relation (3.1) can easily be proven by, e.g. using the Levi Civita formalism. It shows that the defining scalar function of the velocity field Q in eq. (2.35) can be identified with the scalar product $\boldsymbol{\varpi}\cdot\boldsymbol{r}$, which depends on the components of $\boldsymbol{\varpi}$ at $r = R_{\text{CMB}}$ as follows

$$\begin{aligned} Q &= R_{\text{CMB}}\,(\varpi_x \sin\vartheta\,\cos\varphi + \varpi_y \sin\vartheta\,\sin\varphi + \varpi_z\cos\vartheta) \\ &= \frac{R_{\text{CMB}}}{2}\left[\varpi_x\big(e^{i\,\varphi}+e^{-i\,\varphi}\big) + \varpi_y\left(\frac{e^{i\,\varphi}-e^{-i\,\varphi}}{i}\right)\right]\sin\vartheta + R_{\text{CMB}}\,\varpi_z\cos\vartheta \\ &= \frac{R_{\text{CMB}}}{2}\left[e^{i\,\varphi}\,(\varpi_x - i\,\varpi_y) + e^{-i\,\varphi}\,(\varpi_x + i\,\varpi_y)\right]\sin\vartheta + R_{\text{CMB}}\,\varpi_z\cos\vartheta \\ &= \frac{R_{\text{CMB}}}{2}\sqrt{\frac{8\pi}{3}}\left[-Y_{11}\,(\varpi_x - i\,\varpi_y) + Y_{1\,-1}\,(\varpi_x + i\,\varpi_y)\right] + R_{\text{CMB}}\sqrt{\frac{4\pi}{3}}\varpi_z Y_{10} \end{aligned} \tag{3.2}$$

The comparison with the SH expansion of Q results in its non-zero SH coefficients, q_{jk}, in eq. (2.42) being given by:

$$q_{10} = R_c\sqrt{\frac{4\pi}{3}}\varpi_z, \quad q_{11} = -R_{\text{CMB}}\sqrt{\frac{2\pi}{3}}(\varpi_x - i\,\varpi_y), \quad q_{1(-1)} = R_{\text{CMB}}\sqrt{\frac{2\pi}{3}}(\varpi_x + i\,\varpi_y). \tag{3.3}$$

Next, we will determine the topographic height for the surface of an axial rotational ellipsoid, i.e. the departure of this surface from a spherical surface with the radius R_{CMB}, which is assumed to be the minor semi axis, as shown in the sketch below. The equation for its surface is given by

$$\frac{x^2+y^2}{a^2} + \frac{z^2}{b^2} = 1 = \frac{r^2\,\sin^2\vartheta}{a^2} + \frac{r^2\,\cos^2\vartheta}{R^2_{\text{CMB}}} \tag{3.4}$$

from which follows

$$r = \frac{R_{\text{CMB}}}{\sqrt{1-\epsilon^2\sin^2\vartheta}}, \qquad \epsilon^2 = \frac{a^2 - R^2_{\text{CMB}}}{a^2}. \tag{3.5}$$

Due to the fact that ϵ is very small for the core, we can apply a Taylor approximation of first order, obtaining

$$r = R_{\text{CMB}}\,(1 + \frac{1}{2}\epsilon^2\sin^2\vartheta). \tag{3.6}$$

The topographic height h and its non-zero SH coefficients are obtained by comparison of eq. (3.6) with the surface equation (2.3) and the SH expansion, respectively, as

$$h = \frac{R_{\text{CMB}}}{2}\,\epsilon^2\,\sin^2\vartheta = R_{\text{CMB}}\,\epsilon^2\sqrt{\frac{4\pi}{9}}(Y_{00} - \frac{1}{\sqrt{5}}Y_{20}) \quad\Longrightarrow\quad h_{00} = R_{\text{CMB}}\,\epsilon^2\sqrt{\frac{4\pi}{9}}, \quad h_{20} = -R_{\text{CMB}}\,\epsilon^2\sqrt{\frac{4\pi}{45}}, \tag{3.7}$$

where the representations of Y_{20} by $\sin^2\vartheta$ and Y_{00} by $1/\sqrt{4\pi}$ were used (for this expression see Hagedoorn & Geiner-Mai (2008) eqs. A.8 and A.11).

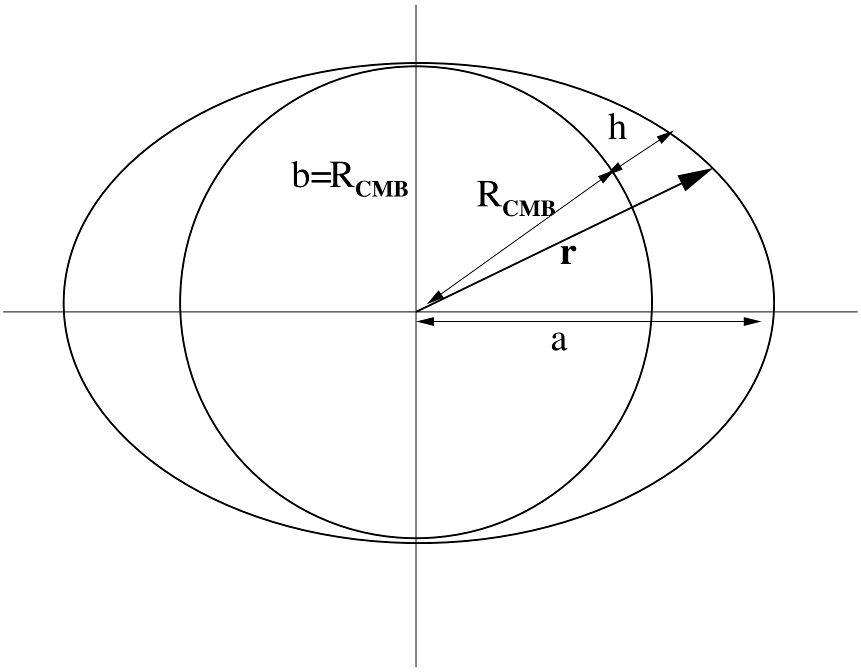

Figure 3.1: Schematic illustration of the axial rotational ellipsoid and its parameters ($\boldsymbol{r}$ = position vector, R_{CMB} = mean core radius as the minor semi axis, h = topographic height with respect to the reference sphere, a = major semi axis)

Now, we can derive the associated torque expressions. The division of the torque in toroidal and poloidal parts is made with respect to that of the velocity field, therefore, a poloidal torque does not exist ($\boldsymbol{u}$ is purely toroidal). The z-component of the toroidal part contains no axial modes and therefore vanishes. The non-zero contributions of h_{jm} to the non-axial torque in eq. (2.49) are those for the pairs $(j = 1, m = -1)$ and $(j = 3, m = -1)$. From eq. (2.49) we then obtain as the topographic torque

$$L^{\mathsf{T}} = -i\, aR_{\text{CMB}}\epsilon^2 \frac{2\sqrt{2\pi}}{15}\left(\frac{2}{\sqrt{3}}\, q_{1(-1)} + 3\sqrt{\frac{6}{7}}\, q_{3(-1)}\right). \tag{3.8}$$

A q_{3m} does not exist [see eq. (3.3)], therefore, the final expression for the complex non-axial torque is given by

$$L^{\mathsf{T}} = -i\, aR_{\text{CMB}}\epsilon^2 \frac{4}{15}\sqrt{\frac{2\pi}{3}}\, q_{1(-1)} = -i\, aR^2_{\text{CMB}}\epsilon^2 \frac{8\pi}{45}(\varpi_x + i\,\varpi_y), \tag{3.9}$$

and its real components by

$$L^{\mathsf{T}}_x = aR^2_{\text{CMB}}\epsilon^2 \frac{8\pi}{45}\,\varpi_y, \qquad L^{\mathsf{T}}_y = -aR^2_{\text{CMB}}\epsilon^2 \frac{8\pi}{45}\,\varpi_x, \qquad a = 2\rho\omega\, R^3_{\text{CMB}}. \tag{3.10}$$

Another choice of the reference sphere (crossing the ellipsoid, allowing also negative values of h) would slightly modify the formulae, but not the magnitude of the torque.

We will now give an estimate of L^{T} using values of the parameters involved in eqs. (3.10); the mean values of which are

$$
\begin{aligned}
\rho &= 10^4\,\text{Kg}\,\text{m}^{-3} && \text{(e.g. Denis et al., 1997)}\\
\omega &= 7.27\times 10^{-5}\,\text{s}^{-1} && \frac{2\pi}{86400\,\text{s}}\\
R_{\text{CMB}} &= 3.485\times 10^6\,\text{m} && \\
a &= 3.494\times 10^6\,\text{m} && \text{flattening}:\ f = \frac{1}{390},\ \text{(e.g. Denis et al., 1997)}\\
\epsilon^2 &= 0.0051 && \text{eq. (3.5).}
\end{aligned} \tag{3.11}
$$

These values give the toroidal torque its scaling factor:

$$\left(L_x^{\mathsf{T}}, L_y^{\mathsf{T}}\right) = 2.13 \times 10^{30}\,\mathrm{Nm\,s} \times (\varpi_y, -\varpi_x). \tag{3.12}$$

In Greiner-Mai (1990), the non-axial components of the vector of relative core rotation are estimated by the frozen-flux approximation. This shows that a representative value for $\omega_{x,y}$ is about $10^{-11}\,\mathrm{s}^{-1}$, and we can conclude that a topographic torque of about 10^{19} Nm is possible in this simple case of a non-axial rigid rotation of the core fluid.

Finally, we will give the scaling unit for the numerical estimation of the torque. If h is measured in km and $\boldsymbol{u}$ in km a^{-1}, then the value of the torque will be 1.95×10^{18} Nm for each 1 km of topography and each $1\,\mathrm{km\,a}^{-1}$ of surface flow velocity. This also shows that values of 10^{19} Nm are possible if the summation over smaller contributions of related modes of h and $\boldsymbol{u}$ is considered.

This consideration shows that the ellipsoidal part of the CMB topography must also be considered, if the CMB tomography inferred from seismic investigations refers to an ellipsoidal reference surface.

Acknowledgments

This work is embedded into the DFG (Deutsche Forschungsgemeinschaft) research unit 584 'Earth Rotation and Global Dynamic Processes', whereby one of the authors is supported by the DFG. For further information, we refer to http://www.erdrotation.de/.

References R

Asari, S., Shimizu, H., Utada, H., 2006. Variability of the topographic core-mantle torque calculated from core surface flow models. Phys. Earth Planet. Inter. 154, 85–111.

Backus, G., 1969. Kinematics of the geomagnetic secular variation in a perfectly conducting core. Phil. Trnas. R. Soc. London A, 263, 239–266.

Ballani, L., Greiner-Mai, H., Stromeyer, D., 2002. Determining the magnetic field in the core-mantle boundary zone by non-harmonic downward continuation. Geophys. J. Int. 149, 374–389.

Bullard, E., Freedman, C., Gellman, H., Nixon, J., 1950. The westward drift of the Earth's magnetic field. Phil. Trans. Roy. Soc. London A, 243, 67–92.

Denis, C., Rogister, Y., Amalvict, M., Delire, C., Denis, A., Munhoven, G., 1997. Hydrostatic flattening, core structure and translational mode of the inner core. Phys. Earth Planet. Inter. 99, 195–206.

Greiner-Mai, H., 1990. The outer core rotation about an inclined axis from geomagnetic secular variations. Astron. Nachr. 311, 317–325.

Greiner-Mai, H., Jochmann, H., Barthelmes, F., Ballani, L., 2003. Possible influence of core processes on the Earth's rotation and the gravity field. J. Geodyn. 36, 343–358.

Hagedoorn, J., Geiner-Mai, H., 2008. Core-Mantle Coupling - Part I: Electromagnetic coupling torques. Sci. Techn. Rep. GFZ Potsdam, STR 08/06 .

Heuser, H., 1993. Lehrbuch der Analysis, Teil 2. B.G. Teubner, Stuttgart.

Hide, R., 1989. Fluctuations in the earth's rotation and the topography of the core-mantle interface. Phil. Trans. Roy. Soc. London A, 328, 351–363.

Hide, R., Boggs, D., Dickey, J., Dong, D., Gross, R., Jackson, A., 1996. Topographic core-mantle coupling and polar motion on decadal time-scales. Geophys. J. Int. 125, 599–607.

Hinderer, J., Legros, H., Gire, H., LeMouël, J.-L., 1987. Geomagnetic secular variation, core motions and implications for the earth's wobble. Phys. Earth Planet. Inter. 59, 329–341.

Jault, D., LeMouël, J.-L., 1989. The topographic torque associated with tangentially geostrophic motion at the core surface and inferences on the flow inside the core. Geophys. Astrophys. Fluid Dyn. 48, 273–396.

Kautzleben, H., 1965. Kugelfunktionen. B.G. Teubner Verlagsgesellschaft, Leipzig.

Krause, F., Rädler, K.-H., 1980. Mean-Field Magnetohydrodynamics and Dynamo Theory. Akademie-Verlag, Berlin.

Morelli, A., Dziewonski, A., 1987. Topography of the core-mantle boundary and lateral homogeneity of the liquid core. Nature 325, 678–683.

Mound, J., Buffett, B., 2007. Viscosity of the earth's fluid core and torsional oscillations. J. Geophys. Res. 112, doi:10.1029/2006JB004426.

Smirnov, W., 1964. Lehrgang der höheren Mathematik, Teil II. VEB Deutscher Verlag der Wissenschaften.

Steinberger, B., Holme, R., 2008. Mantle flow models with core-mantle boundary constraints and chemical heterogeneities in the lowermost mantle. J. Geophys. Res. 113, doi:10.1029/2007JB005080.

Sze, E., van der Hilst, R., 2003. Core mantle boundary topography from short period PcP, PKP and PKKP data. Phys. Earth Plant. Inter. 135, 27–46.

Varshalovich, D., Moskalev, A., Khersonskii, V., 1989. Quantum Theory of Angular Momentum. World Scientific, Singapore.

Wardinski, I., 2005. Core surface flow models from decadal and subdecadal secular variation of the main geomagnetic field. Sci. Techn. Rep. GFZ Potsdam, STR 05/07 .

Wardinski, I., Holme, R., 2006. A time-dependent model of the earth's magnetic field and its secular variation for the period 1980 – 2000. J. Geophys. Res. 111, doi:10.1029/2006JB004401.

Spherical harmonic (SH) functions | A

The fully normalized SH functions according to Varshalovich et al. (1989) and some relations between them are shown in Hagedoorn & Geiner-Mai (2008). In this report, we will repeat some basic relations and derive the expressions used in section 2.2 for the torque components.

The scalar spherical harmonics, Y_{jm}, of degree j and order m are defined by:

$$Y_{jm}(\Omega) := P_{jm}(\cos\vartheta)\, e^{i\,m\varphi} \tag{A.1}$$

where $i = \sqrt{-1}$, $\Omega = (\vartheta, \varphi)$ and P_{jm} are the associated Legendre-polynomials, which are orthonormal on the unit sphere,

$$\int\limits_{\Omega_0} Y_{jm}(\Omega) Y^*_{j'm'}(\Omega)\, \mathrm{d}\Omega = \delta_{jm}\delta_{j'm'}. \tag{A.2}$$

δ_{jm} is the Kronecker's symbol and the asterix $*$ denotes the complex conjugate,

$$Y^*_{jm}(\Omega) = (-1)^m\, Y_{j\,-m}(\Omega). \tag{A.3}$$

For our derivations, we also need the transformation between fully othonormal Legendre-polynomials, P_{jm} and the Ferrers-Neuman representations, $\widetilde{P}_{jm}$. This is given by:

$$\widetilde{P}_{jm}(\cos\vartheta) = \lambda_{jm}\, P_{jm}(\cos\vartheta) \tag{A.4}$$

with

$$\lambda_{jm} = (-1)^m \sqrt{\frac{4\pi}{2j+1}\frac{(j+m)!}{(j-m)!}}, \tag{A.5}$$

To solve the integrals in eqs. (2.43)-(2.46) by applying the normalization condition (A.2), we require some relations between the SH functions, which we will derive here. Those are not standard according to Varshalovich et al. (1989), therefore, we use some expressions from Kautzleben (1965) that are valid for the Legendre-polynomials in Ferrers-Neumann normalization and transform them back to the fully normalized representations by using the definition (A.1) and the transformations (A.4) and (A.5). For the toroidal z-component of the torque in eq. (2.45), the derivation of the needed relations between SH functions is given by

$$\begin{aligned}
\cos\vartheta\, Y_{jm} &= e^{i\,m\varphi}\, \lambda^{-1}_{jm} \big(\cos\vartheta\, \widetilde{P}_{jm}\big) \\
&= e^{i\,m\varphi}\, \lambda^{-1}_{jm} \left[\frac{j-m+1}{2j+1}\, \widetilde{P}_{(j+1)m} + \frac{j+m}{2j+1}\, \widetilde{P}_{(j-1)m}\right] \\
&= e^{i\,m\varphi} \left[\frac{\lambda_{(j+1)m}}{\lambda_{jm}}\frac{j-m+1}{2j+1}\, \widetilde{P}_{(j+1)m} + \frac{\lambda_{(j-1)m}}{\lambda_{jm}}\frac{j+m}{2j+1}\, \widetilde{P}_{(j-1)m}\right] \\
&= \left[\frac{\lambda_{(j+1)m}}{\lambda_{jm}}\frac{j-m+1}{2j+1}\, Y_{(j+1)m} + \frac{\lambda_{(j-1)m}}{\lambda_{jm}}\frac{j+m}{2j+1}\, Y_{(j-1)m}\right]
\end{aligned} \tag{A.6}$$

where the second line is obtained according to Kautzleben (1965, eq. 256a). The λ-factors can be evaluated according to eq. (A.5) [4π and $(-1)^m$ cancel out]

$$\frac{\lambda_{(j+1)m}}{\lambda_{jm}} = \sqrt{\frac{(2j+1)(j+m+1)!(j-m)!}{(2j+3)(j-m+1)!(j+m)!}} = \sqrt{\frac{(2j+1)(j+m+1)}{(2j+3)(j-m+1)}}, \tag{A.7}$$

$$\frac{\lambda_{(j-1)m}}{\lambda_{jm}} = \sqrt{\frac{(2j+1)(j+m-1)!(j-m)!}{(2j-1)(j-m-1)!(j+m)!}} = \sqrt{\frac{(2j+1)(j-m)}{(2j-1)(j+m)}}. \tag{A.8}$$

Applying (A.7) and (A.8) to eq. (A.6) gives

$$\cos\vartheta\, Y_{jm} = \sqrt{\frac{(j+1)^2-m^2}{(2j+1)(2j+3)}}Y_{(j+1)m} + \sqrt{\frac{j^2-m^2}{(2j+1)(2j-1)}}Y_{(j-1)m} \tag{A.9}$$

To derive the relation for the axial poloidal torque (2.46), we use the formula (A.21) derived by Hagedoorn & Geiner-Mai (2008):

$$\sin\vartheta\,\frac{\partial}{\partial\vartheta}Y_{jm} = j\sqrt{\frac{(j+1)^2-m^2}{(2j+1)(2j+3)}}Y_{(j+1)m} - (j+1)\sqrt{\frac{j^2-m^2}{(2j+1)(2j-1)}}Y_{(j-1)m}. \tag{A.10}$$

The necessary relation is then obtained, if we apply (A.9) to (A.10)

$$\begin{aligned}
\cos\vartheta\,\sin\vartheta\,\frac{\partial}{\partial\vartheta}Y_{jm} &= j\sqrt{\frac{(j+1)^2-m^2}{(2j+1)(2j+3)}}\left(\cos\vartheta\,Y_{(j+1)m}\right) - (j+1)\sqrt{\frac{j^2-m^2}{(2j+1)(2j-1)}}\left(\cos\vartheta\,Y_{(j-1)m}\right)\\
&= j\sqrt{\frac{(j+1)^2-m^2}{(2j+1)(2j+3)}}\left[\sqrt{\frac{(j+2)^2-m^2}{(2j+3)(2j+5)}}Y_{(j+2)m} + \sqrt{\frac{(j+1)^2-m^2}{(2j+1)(2j+3)}}\,Y_{jm}\right]\\
&- (j+1)\sqrt{\frac{j^2-m^2}{(2j-1)(2j+1)}}\left[\sqrt{\frac{j^2-m^2}{(2j-1)(2j+1)}}Y_{jm} + \sqrt{\frac{(j-1)^2-m^2}{(2j-1)(2j-3)}}\,Y_{(j-2)m}\right]
\end{aligned} \tag{A.11}$$

from which follows

$$\begin{aligned}
\cos\vartheta\,\sin\vartheta\,\frac{\partial}{\partial\vartheta}Y_{jm} &= \frac{j}{2j+3}\sqrt{\frac{[(j+2)^2-m^2][(j+1)^2-m^2]}{(2j+1)(2j+5)}}Y_{(j+2)m}\\
&- \frac{(j+1)}{2j-1}\sqrt{\frac{[j^2-m^2][(j-1)^2-m^2]}{(2j+1)(2j-3)}}Y_{(j-2)m}\\
&\frac{1}{2j+1}\left(\frac{j[(j+1)^2-m^2]}{(2j+3)} - \frac{(j+1)(j^2-m^2)}{(2j-1)}\right)Y_{jm}
\end{aligned} \tag{A.12}$$

which is used to solve the integral in eq. (2.46).

To derive the relation for the equatorial toroidal torque (2.43), we transform the integrand to $\widetilde{P}_{jm}$ and use eq. (260a) from Kautzleben (1965) to express $\partial Y_{jm}/\partial\vartheta$ by SH functions, as follows

$$\begin{aligned}
\left(m\,\cot\vartheta\,Y_{jm} - \frac{\partial}{\partial\vartheta}Y_{jm}\right)e^{i\,\varphi}\,\cos\vartheta &= \left[\left(m\,\cot\vartheta\,P_{jm} - \frac{\partial}{\partial\vartheta}P_{jm}\right)\,\cos\vartheta\right]e^{i\,(m+1)\varphi}\\
&= \frac{e^{i\,(m+1)\varphi}}{\lambda_{jm}}\left(m\,\cot\vartheta\,\widetilde{P}_{jm} - \frac{\partial}{\partial\vartheta}\widetilde{P}_{jm}\right)\,\cos\vartheta\\
&= \frac{e^{i\,(m+1)\varphi}}{\lambda_{jm}}\widetilde{P}_{j(m+1)}\,\cos\vartheta\\
&= \frac{\lambda_{j(m+1)}}{\lambda_{jm}}Y_{j(m+1)}\,\cos\vartheta\\
&= -\sqrt{(j-m)(j+m+1)}Y_{j(m+1)}\,\cos\vartheta.
\end{aligned} \tag{A.13}$$

To involve the cos-function, we apply the relation (A.9) and obtain

$$\begin{aligned}
\left(m\,\cot\vartheta\,Y_{jm} - \frac{\partial}{\partial\vartheta}Y_{jm}\right)e^{i\,\varphi}\,\cos\vartheta &= -\sqrt{(j-m)(j+m+1)}Y_{j(m+1)}\,\cos\vartheta\\
&= -\left[(j-m)\sqrt{\frac{(j+m+2)(j+m+1)}{(2j+1)(2j+3)}}Y_{(j+1)(m+1)}\right.\\
&\left.+(j+m+1)\sqrt{\frac{(j-m)(j-m-1)}{(2j+1)(2j-1)}}Y_{(j-1)(m+1)}\right].
\end{aligned} \tag{A.14}$$

To derive the relation for the equatorial poloidal torque (2.44), we modify at first eq. (260a) in Kautzleben (1965). From this equation,

$$\sin\vartheta \frac{\partial}{\partial\vartheta}\tilde{P}_{jm} = m\,\cos\vartheta\,\tilde{P}_{jm} - \sin\vartheta\,\tilde{P}_{j(m+1)}, \tag{A.15}$$

which we multiplying by $\cos\vartheta\,\sin^{-1}\vartheta$ follows that

$$\begin{aligned} \cos\vartheta \frac{\partial}{\partial\vartheta}\tilde{P}_{jm} &= m\,\frac{\cos^2\vartheta}{\sin\vartheta}\,\tilde{P}_{jm} - \cos\vartheta\,\tilde{P}_{j(m+1)} \\ &= \frac{m}{\sin\vartheta}\,\tilde{P}_{jm} - m\,\sin\vartheta\,\tilde{P}_{jm} - \cos\vartheta\,\tilde{P}_{j(m+1)}, \end{aligned} \tag{A.16}$$

so that we find for the integrand in eq. (2.44)

$$\begin{aligned} A_{jm} &= \left[\cos\vartheta\,\frac{\partial}{\partial\vartheta}Y_{jm} - \frac{m}{\sin\vartheta}Y_{jm}\right] e^{i\,\varphi}\,\cos\vartheta \\ &= \frac{e^{i\,(m+1)\varphi}}{\lambda_{jm}}\left[\cos\vartheta\frac{\partial}{\partial\vartheta}\tilde{P}_{jm} - \frac{m}{\sin\vartheta}\,\tilde{P}_{jm}\right]\,\cos\vartheta \\ &= -\frac{e^{i\,(m+1)\varphi}}{\lambda_{jm}}\left(m\,\sin\vartheta\,\tilde{P}_{jm} + \cos\vartheta\,\tilde{P}_{j(m+1)}\right)\,\cos\vartheta. \end{aligned} \tag{A.17}$$

Applying eqs. (257a) and (259a) of Kautzleben (1965) gives

$$\begin{aligned} A_{jm} &= -\frac{e^{i\,(m+1)\varphi}}{\lambda_{jm}}\frac{1}{2j+1}\Bigg(m\left[\tilde{P}_{(j+1)(m+1)} - \tilde{P}_{(j-1)(m+1)}\right] \\ &\quad + (j-m)\tilde{P}_{(j+1)(m+1)} + (j+m+1)\tilde{P}_{(j-1)(m+1)}\Bigg)\cos\vartheta \\ &= -\frac{e^{i\,(m+1)\varphi}}{(2j+1)\lambda_{jm}}\left[j\,\tilde{P}_{(j+1)(m+1)} + (j+1)\,\tilde{P}_{(j-1)(m+1)}\right]\,\cos\vartheta. \end{aligned} \tag{A.18}$$

Applying eq. (259a) of Kautzleben (1965) for the product of $\widetilde{P}_{\dots}$ and $\cos$ again, and using the back transformation according to eq. (A.3) gives

$$\begin{aligned} A_{jm} &= \frac{j(j-m+1)\,\lambda_{(j+2)(m+1)}}{(2j+1)(2j+3)\lambda_{jm}}\,Y_{(j+2)(m+1)} \\ &\quad - \frac{(j+1)(j+m)\,\lambda_{(j-2)(m+1)}}{(2j-1)(2j+1)\lambda_{jm}}\,Y_{(j-2)(m+1)} \\ &\quad - \frac{\lambda_{j(m+1)}}{(2j+1)\lambda_{jm}}\left[\frac{j(j+m+2)}{2j+3} + \frac{(j+1)(j-m-1)}{2j-1}\right]Y_{j(m+1)}. \end{aligned} \tag{A.19}$$

Evaluating the ratio of the λ-factors according to eq. (A.5) gives the final expression

$$\begin{aligned} A_{jm} &= \frac{j}{2j+3}\sqrt{\frac{[(j+1)^2-m^2][j+m+2][j+m+3]}{(2j+1)(2j+5)}}\,Y_{(j+2)(m+1)} \\ &\quad + \frac{(j+1)}{2j-1}\sqrt{\frac{[j^2-m^2][j-m-1][j-m-2]}{(2j+1)(2j-3)}}\,Y_{(j-2)(m+1)} \\ &\quad + \frac{\sqrt{(j-m)(j+m+1)}}{2j+1}\left[\frac{j(j+m+2)}{2j+3} + \frac{(j+1)(j-m-1)}{2j-1}\right]Y_{j(m+1)}. \end{aligned} \tag{A.20}$$

List of symbols | L

Symbol	Explanation	Page
a	major semi-axis of the core-mantle boundary (CMB) approx. ellipsoid	15
b	minor semi-axis of the core-mantle boundary (CMB) approx. ellipsoid	15
$\boldsymbol{B}$	magnetic flux vector	7
$\boldsymbol{B}^{\mathsf{P}}$	poloidal magnetic flux	7
$\boldsymbol{B}^{\mathsf{T}}$	toroidal magnetic flux	7
$\mathrm{d}S$	infinitesimal surface element	3
$\mathrm{d}V$	infinitesimal volume element	3
$\mathrm{d}\Omega$	infinitesimal surface element (in spherical coordinates)	4
$\boldsymbol{e}_i$	unit-base vector	3
f	Coriolis parameter	8
$\boldsymbol{F}$	geomertical surface of the CMB	3
$\boldsymbol{g}$	gravitational acceleration	7
h	topographic height of the CMB (with respect to a reference sphere)	3
h_{jm}	SH coefficient of h	12
$\boldsymbol{j}$	electric current density	7
$\boldsymbol{L}$	topographic core-mantle coupling (TOP) torque	3
L^{P}	complex combination of non-axial components of the poloidal TOP torque	11
L_z^{P}	axial component of the poloidal TOP torque	11
L^{T}	complex combination of non-axial components of the toroidal TOP torque	11
L_z^{T}	axial component of the toroidal TOP torque	11
$\boldsymbol{n}$	outward normal unit vector	3
$\boldsymbol{N}$	normal vector on CMB topography $\boldsymbol{F}$	3
p	total pressure in the outer core fluid	7
p_{u}	dynamic pressure of outer core fluid	3
p_{jm}	SH coefficient of P	12
P	defining scalar function of $\boldsymbol{u}^{\mathsf{P}}$	11
$P_{jm}(\cos\vartheta)$	associated Legendre function	12
$\tilde{P}_{kl}(\cos\vartheta)$	associated Legendre function in Ferrers-Neumann normalization	21
q_{jm}	SH coefficient of Q	12
Q	defining scalar function of $\boldsymbol{u}^{\mathsf{T}}$	11
$\boldsymbol{r}$	position vector	3
R_{CMB}	radius of the CMB reference sphere	3
$\boldsymbol{u}$	fluid-flow velocity of the outer core fluid	7
$\boldsymbol{u}_{\mathsf{H}}$	tangential part of $\boldsymbol{u}$	8
$\boldsymbol{u}^{\mathsf{P}}$	poloidal part of $\boldsymbol{u}$	11
$\boldsymbol{u}^{\mathsf{T}}$	toroidal part of $\boldsymbol{u}$	11
x, y, z	geocentric, mantle-fixed Cartesian coordinates	11
$Y_{jm}(\Omega)$	orthonormal scalar spherical harmonics	12
ϵ	ellipticity of the CMB	15
ϑ	spherical coordinate: co-latitude	3
λ_{jm}	normalization factor between different Legendre functions	21
ν	dynamic viscosity	7
ρ	volume mass density	7
φ	spherical coordinate: longitude	3
$\boldsymbol{\omega}$	angular velocity relative to inertial frame	7
$\boldsymbol{\varpi}$	angular velocity of the core fluid in mantle-fixed coordinate system	15
Ω	$:= (\vartheta, \varphi)$	4
∇	nabla operator	3
∇_{H}	tangential part of the nabla operator	4

ISSN 1610-0956